Structural Evolution of Small Gold Clusters Doped by One and Two Boron Atoms

Rafael Grande-Aztatzi,[a] Paulina R. Martínez-Alanis,[b] José Luis Cabellos,[a] Edison Osorio,[c] Ana Martínez,*[b] and Gabriel Merino*[a]

The potential energy surfaces (PES) of a series of gold–boron clusters with formula Au_nB ($n = 1–8$) and Au_mB_2 ($m = 1–7$) have been explored using a modified stochastic search algorithm. Despite the complexity of the PES of these clusters, there are well-defined growth patterns. The bonding of these clusters is analyzed using the adaptive natural density partitioning and the natural bonding orbital analyses. Reactivity is studied in terms of the molecular electrostatic potential. © 2014 Wiley Periodicals, Inc.

DOI: 10.1002/jcc.23748

Introduction

Gold clusters are important due to the potential applications in medicine, catalysis, and plasmonic materials.[1] Considering that gold is an inert solid, one of the most attractive properties of the gold clusters is its capability to be reactive.[2] For example, gold clusters are able to catalyze the CO oxidation.[3] Considerable efforts have been devoted to explain the factors that contribute to the extraordinary catalytic activity of gold clusters, including the relationship between structure and reactivity.[1g,4] In particular, theoretical studies of small gold clusters indicate that up to nine gold atoms, the planar structures are the most stable ones.[5,6] Between nine and 16 atoms, both two-dimentional (2D) and three-dimentional (3D) can coexist. After 16 gold atoms, the 3D arrangements are prevailing.[5m,7,8] The reactivity of these clusters is related to the structure; thus, 2D gold clusters could react different to their 3D congeners. For this reason, the correct structural characterization of gold clusters is critical.

Doping a gold cluster can induce modifications into its structure and properties.[9] Particularly, gold–boron clusters caught our attention because in principle no drastic structural changes respect to the pure gold clusters were reported.[9f] However, photoelectron spectroscopic studies indicate an opposite behavior. Recently, two of us reported that the structures of Au_nB ($n = 2–8$) clusters[9f] are mainly planar and better electron donors than pure gold clusters, being the B atoms the active sites. So, there is a reactivity increase of the gold clusters due to the presence of a boron atom. However, the number of candidates used for the global minimum search was quite limited. So, it is required to expand or improve the way of doing the potential energy surfaces (PES) analysis.

Herein, we explore in detail the PES of the Au_nB ($n = 1–8$) and Au_mB_2 ($m = 1–7$) clusters using a modified stochastic search algorithm. The bonding of these clusters is analyzed using the adaptive natural density partitioning (AdNDP)[10] and the natural bonding orbital[11] analyses. Reactivity is studied in terms of the molecular electrostatic potential. Our computations show that such gold–boron clusters have complex PESs, with several structures having similar stability and probably different reactivity, but there are well-defined growth patterns.

Computational Details

A modified Kick heuristic called Bilatu[12] is used to explore in detail the PES of the first two spin multiplicities of the title systems. This procedure starts with the random generation of the atomic positions using the Mersenne twister algorithm.[13] The selected structures must achieve three conditions:

1. All the atomic positions are located into a sphere of radius R, where R is the sum of the covalent radii of all the atoms.
2. The distance between any pair of atoms must be longer than the sum of their covalent radii.
3. Each atom should be connected at least to one atom. Such condition is achieved using the Laplacian matrix.

[a] *R. Grande-Aztatzi, J. L. Cabellos, G. Merino*
Departamento de Física Aplicada, Centro de Investigación y de Estudios Avanzados Unidad Mérida, Km. 6 Antigua carretera a Progreso A.P. 73, Cordemex 97310, Mérida, Yucatán, México
E-mail: gmerino@mda.cinvestav.mx

[b] *P. R. Martínez-Alanis, A. Martínez*
Instituto de Investigaciones en Materiales, Universidad Nacional Autónoma de México, Circuito Exterior s/n C.U., P.O.Box 70-360, Coyoacán 04510, México City, D.F., México
E-mail: martina@unam.mx

[c] *Edison Osorio*
Departamento de Ciencias Básicas, Fundación Universitaria Luis Amigó, SISCO, Transversal, 51A # 67B 90, Medellín, Colombia.

Contract grant sponsor: Moshinsky Foundation (Mérida; Contract grant sponsor: Conacyt (Mérida); Contract grant number: INFRA-2013-01-204586; Contract grant sponsors: DGAPA-PAPIIT (UNAM) and Instituto de Investigaciones en Materiales.

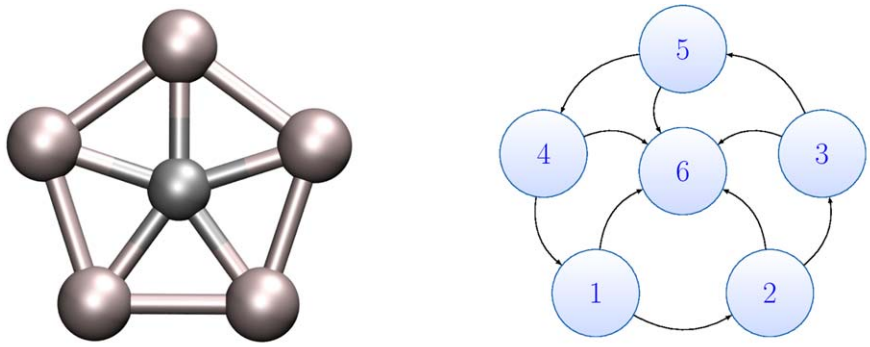

$$\mathbf{L}=\begin{pmatrix} \mathbf{3} & -1 & 0 & -1 & 0 & -1 \\ -1 & \mathbf{3} & -1 & 0 & 0 & -1 \\ 0 & -1 & \mathbf{3} & 0 & -1 & -1 \\ -1 & 0 & 0 & \mathbf{3} & -1 & -1 \\ 0 & 0 & -1 & -1 & \mathbf{3} & -1 \\ -1 & -1 & -1 & -1 & -1 & \mathbf{5} \end{pmatrix};\ \mathbf{D}=\begin{pmatrix} \mathbf{3} & 0 & 0 & 0 & 0 & 0 \\ 0 & \mathbf{3} & 0 & 0 & 0 & 0 \\ 0 & 0 & \mathbf{3} & 0 & 0 & 0 \\ 0 & 0 & 0 & \mathbf{3} & 0 & 0 \\ 0 & 0 & 0 & 0 & \mathbf{3} & 0 \\ 0 & 0 & 0 & 0 & 0 & \mathbf{5} \end{pmatrix};\ \mathbf{A}=\begin{pmatrix} \mathbf{0} & 1 & 0 & 1 & 0 & 1 \\ 1 & \mathbf{0} & 1 & 0 & 0 & 1 \\ 0 & 1 & \mathbf{0} & 0 & 1 & 1 \\ 1 & 0 & 0 & \mathbf{0} & 1 & 1 \\ 0 & 0 & 1 & 1 & \mathbf{0} & 1 \\ 1 & 1 & 1 & 1 & 1 & \mathbf{0} \end{pmatrix}$$

Figure 1. An example of a labeled graph and its Laplacian matrix.

Given a graph *G* with *n* vertices, its Laplacian matrix **L** is defined as: **L** = **D** − **A**, where **D** is the degree matrix and **A** is the adjacency matrix. **D** is a diagonal matrix, which contains information about the coordination number of each atom. An adjacency matrix is a means of representing which vertices of a graph are adjacent to which other vertices. The adjacency matrix is a square matrix whose elements are given by:

$$A_{ij}=\begin{cases} 1 & \text{if the atom i is connected to atom } j \\ 0 & \text{otherwise} \end{cases}$$

In a chemical sense, it represents a connectivity matrix. Figure 1 depicts an example of a labeled molecular graph and its corresponding Laplacian matrix.

The number of times zero appears as an eigenvalue in the Laplacian is the number of connected components in the graph. In our particular case, all the atoms in the initial structures should be connected, that is, if more than one zero appears as eigenvalues in the Laplacian matrix then the structure is removed.

If these three conditions are satisfied then the structure is optimized. For each atom into the cluster, 100 structures are proposed. For instance, 800 different structures are initially generated for Au_7B.

A geometrical comparison among all the optimized structures is performed to select the different candidates for the final geometry optimization at a higher level of theory. In our case, the preoptimization is done at the PBE0/LANL2DZ[14] level and the final reoptimization and characterization at the PBE0/def2-TZVP[4a,15] level. All computations are carried out using Gaussian 09 program.[16]

The chemical bond is analyzed in terms of the AdNDP method,[10] recently developed and implemented by Zubarev and Boldyrev. The AdNDP approach leads to partitioning of the charge density into elements with the lowest possible number of atomic centers per electron pair: *n*-center-two-electron (*n*c–2e) bonds, including core electrons, lone pairs, 2c–2e bonds, and so on. AdNDP accepts only those bonding elements whose occupation numbers (ON) exceed the specified threshold values, which are usually chosen to be close to 2.00 |e|.

Structures of Au_nB (n = 1–8)

Local minima of the Au_nB (n = 1–5) clusters found within 15 kcal/mol above the global minimum structure are shown in Figure 2. Local minima higher in energy were also located, but they are not included in the discussion. Only one minimum in the selected range is present for clusters up to three gold atoms. In the case of Au_4B and Au_5B, there are three and two local minima, respectively. Note that low spin states are favored.

Li and Li have analyzed in detail the first four clusters of this series via B3LYP/SDD computations.[17] The global minimum structures computed at the PBE0/def2-TZVP are in agreement to those computed at the B3LYP/SDD level. Previously, a planar C_{2v} structure (Au_4B_**4**) was suggested as the lowest lying isomer at the B3LYP/LANL2DZ level,[9f] but the smallest frequency computed at that level was only 7 cm^{-1}. Au_4B_**4** is higher in energy than the lowest lying structure reported here; the relative energy of Au_4B_**4** with respect to the global minimum is 12.2 kcal/mol at the PBE0/def2-TZVP level. At the B3LYP/LANL2DZ level, Au_4B_**4** is also less stable than Au_4B_**1** by 9.5 kcal/mol. Actually there are two structures lower in energy than Au_4B_**4** (See Fig. 2). Following the imaginary frequency, Au_4B_**4** converged to the global minimum. Our computations show that Au_4B adopts a D_{2d} structure in agreement with the results of Li et al.[17]

For Au_5B, there are no planar structures in a range of 15 kcal/mol. The global minimum form is a C_{4v} square-based

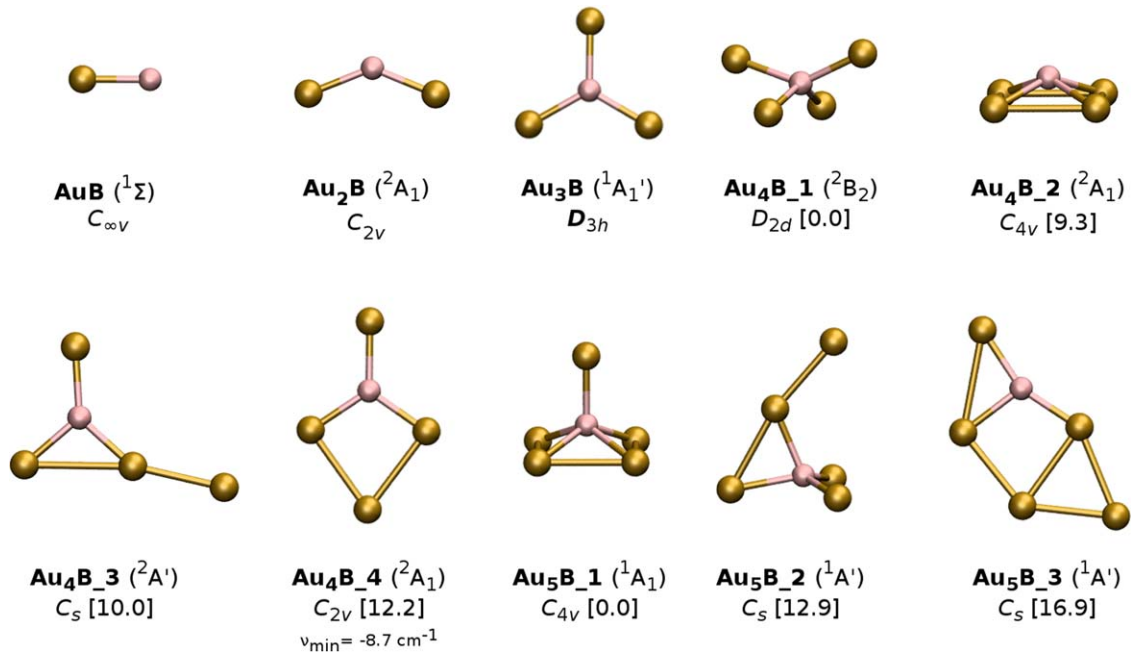

Figure 2. Isomers of the Au_nB ($n = 1$–4) clusters in a range of 15 kcal/mol respect to the corresponding global minimum. The energy differences (in brackets) include the zero point energy correction.

pyramid (Au_5B_**1**) with a pentacoordinate boron atom. The Au—B bond lengths (2.00 and 2.11 Å for the apical and equatorial bonds, respectively) are longer than those found for the smaller clusters. The most stable planar form (Au_5B_**3**), suggested as the global minimum by Romero et al., is 16.9 kcal/mol less stable than the lowest lying structure found here.[9f] Note that the structures in Figure 2 were not considered by Romero et al. as candidates, since in that study the construction of initial candidates was done substituting one gold atom by boron. Due to the planarity of gold clusters, the resulting structures of gold–boron clusters were also planar.

Figure 3 depicts nine different isomers for Au_6B, both planar and 3D. In a previous report, the structure labeled as Au_6B_**3** was classified as the ground state.[9f] According to the results reported here, this is 6.9 kcal/mol less stable than the most stable structure. The global minimum is the result of a gold atom interacting to the square-based pyramid of Au_5B_**1**.

The optimized structures of Au_7B are reported in Figure 4. There are eight different geometries in a range of 15 kcal/mol. The most obvious form derived from the interaction of two gold atoms with Au_5B_**1** (Au_7B_**2**) is not the global minimum. The ground state is a planar structure, resulting from the addition of a gold atom to Au_6B_**3** around the boron to form a planar tetracoordinate boron atom (Au_7B_**1**). This is the same ground state reported before by Romero et al. Notice that the relative energy between the two first isomers of Au_7B is less than 3 kcal/mol. So, both structures could be detected experimentally.

Figure 5 depicts 20 isomers found for Au_8B again in a range of 15 kcal/mol. Structures Au_8B_**1**, Au_8B_**3**, Au_8B_**8**, Au_8B_**9**, and Au_8B_**11** are derived from the Au_7B_**1** skeleton, where an extra gold atom interacts in different positions. Note that the most stable form possesses a pentacoordinate boron atom (Au_8B_**1**). The planar structure labeled as Au_8B_**5** was reported before as the ground state, but it is 8.9 kcal/mol less stable than Au_8B_**1**.

The structural evolution from Au_4B to Au_8B can be understood by looking similarities into their geometries. For the 3D structures, Au_4B_**1** or Au_4B_**2** plus one gold atom gives Au_5B_**1**. One extra gold atom generates Au_6B_**1**. This 3D form is similar to Au_7B_**2**, but this is not the global minimum for such stoichiometry. The core structure of Au_4B is maintained in Au_8B_**2**, but it is 6.8 kcal/mol less stable than the corresponding ground state. Conversely, if we follow the growth pattern of planar structures starting from Au_3B, it is possible to obtain Au_4B_**3**, Au_5B_**3**, Au_6B_**3**, Au_7B_**1**, and, finally, Au_8B_**4**. In summary, 3D arrangements dominate the Au_nB ($n = 4$–8) stoichiometries.

Structures of Au_mB_2 (m = 1–7)

Now, let us discuss about the structural changes induced by the insertion of one additional boron atom. Figure 6 summarizes the results for Au_mB_2 with $m = 1$–7. Figures 1-SI to 4-SI contain the local minima found in the range of 15 kcal/mol for each stoichiometry. Every structure in Figure 6 has a B—B bond. Actually, in the selected range of energy, there is not a local minimum without a B—B bond. This is expected because the B—B bond dissociation energy is around 3 eV whilst the Au—Au bond dissociation energy is only 2.3 eV. Quite recently, Castro et al. reported a similar behavior for B_2P_5 clusters, where all the local minima in a range of 20 kcal/mol show a B—B bond.[18]

In 2010, Yao et al. reported a detailed structural analysis of the Au_mB_2 ($m = 1$, 3, 5).[19] In our case, the global minima for these three stoichiometries are the same. The ground state for AuB_2 corresponds to a quartet state with a linear structure

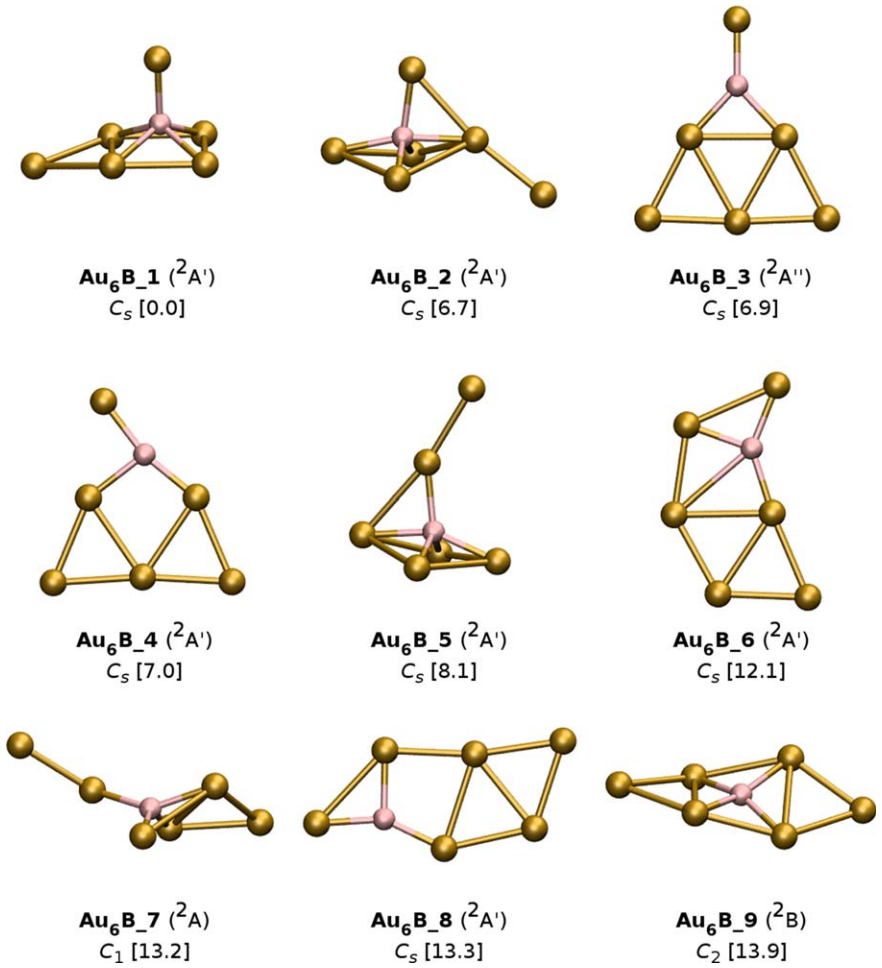

Figure 3. Isomers of the Au_6B clusters in a range of 15 kcal/mol respect to the corresponding global minimum. The energy differences (in brackets) include the zero point energy correction. [Color figure can be viewed in the online issue, which is available at wileyonlinelibrary.com.]

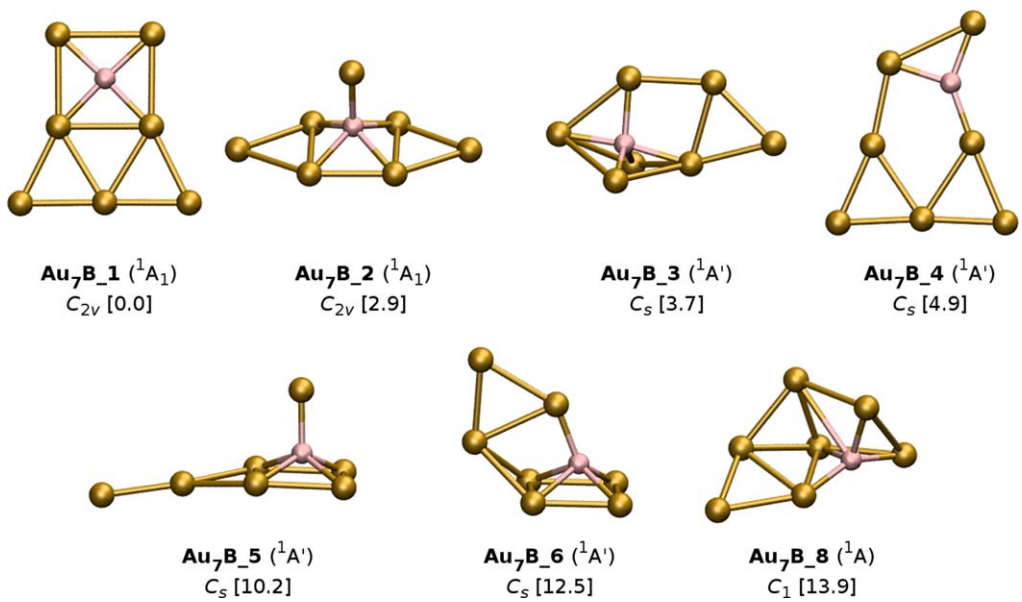

Figure 4. Isomers of the Au_7B clusters in a range of 15 kcal/mol respect to the corresponding global minimum. The energy differences (in brackets) include the zero point energy correction. [Color figure can be viewed in the online issue, which is available at wileyonlinelibrary.com.]

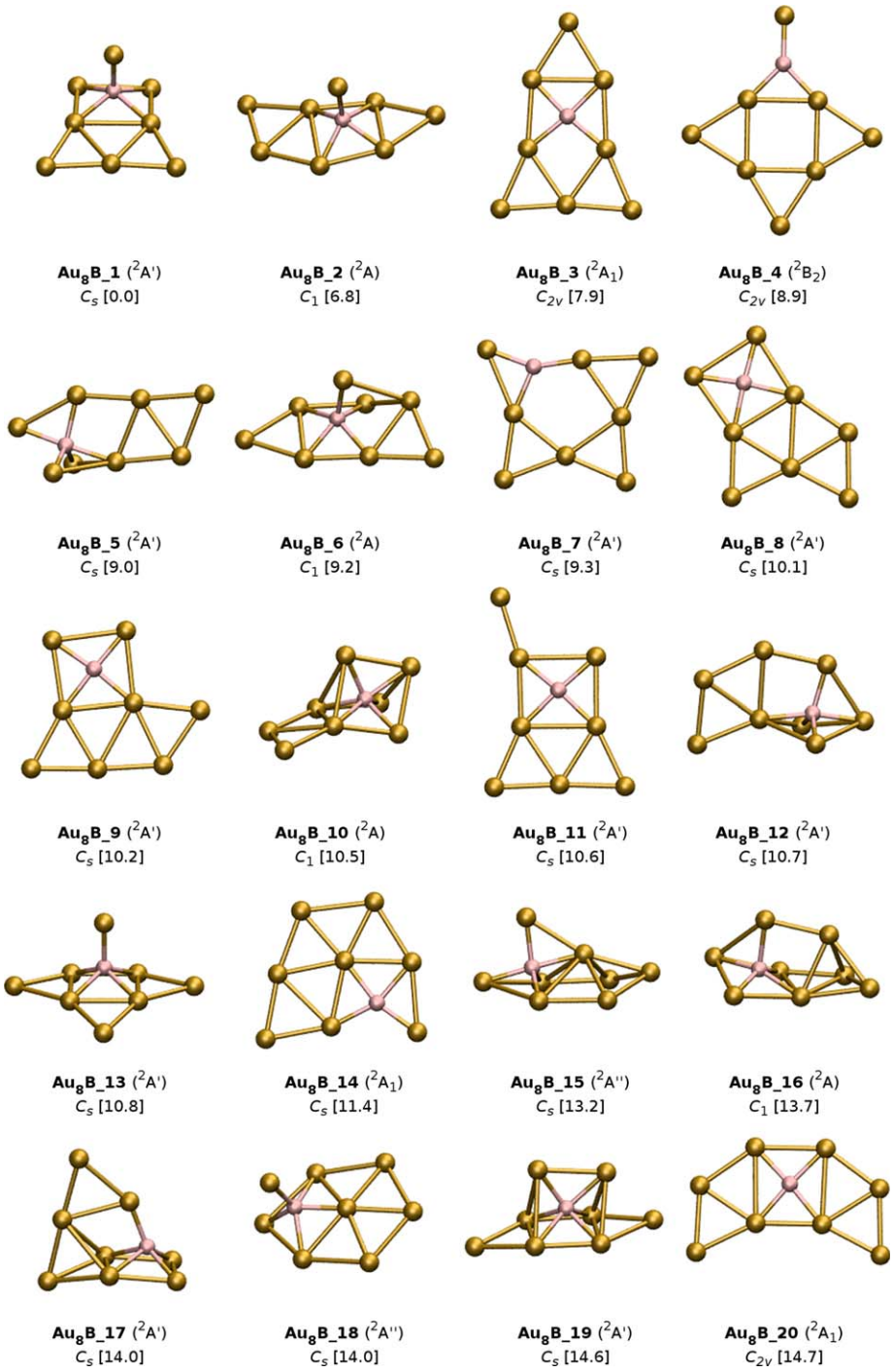

Figure 5. Isomers of the Au_8B clusters in a range of 15 kcal/mol respect to the corresponding global minimum. The energy differences (in brackets) include the zero point energy correction. [Color figure can be viewed in the online issue, which is available at wileyonlinelibrary.com.]

(AuB_2_**1**). Au_2B_2 also adopts a linear form with a triplet state configuration. This is opposite to the small Au_nB clusters, where the low spin forms dominate. In the rest of the studied Au_mB_2 clusters, low spin states are favored.

Clearly, the 3D structures are more stable than the planar ones for the Au_mB_2 ($m = 4$–7) clusters. Except Au_6B_2, the boron atoms are tetracoordinated. Au_6B_2 has an exceptional structure with a pentacoordinate boron atom. A pentacoordinate boron atom is also found in Au_5B_2_**2**, which is only 0.4 kcal/mol less stable than the corresponding global minimum. In the case of Au_5B_2, obviously both isomers could be detected experimentally. So, the substitution of two gold atoms by boron changes drastically the structure of the original gold clusters. Conversely, the B—B bond will survive independently of the number of gold atoms that form the cluster.

Bonding Analysis

Gold (2.54) is more electronegative than boron (2.04) due to relativistic effects.[20] This is the reason why in the AuB dimer,

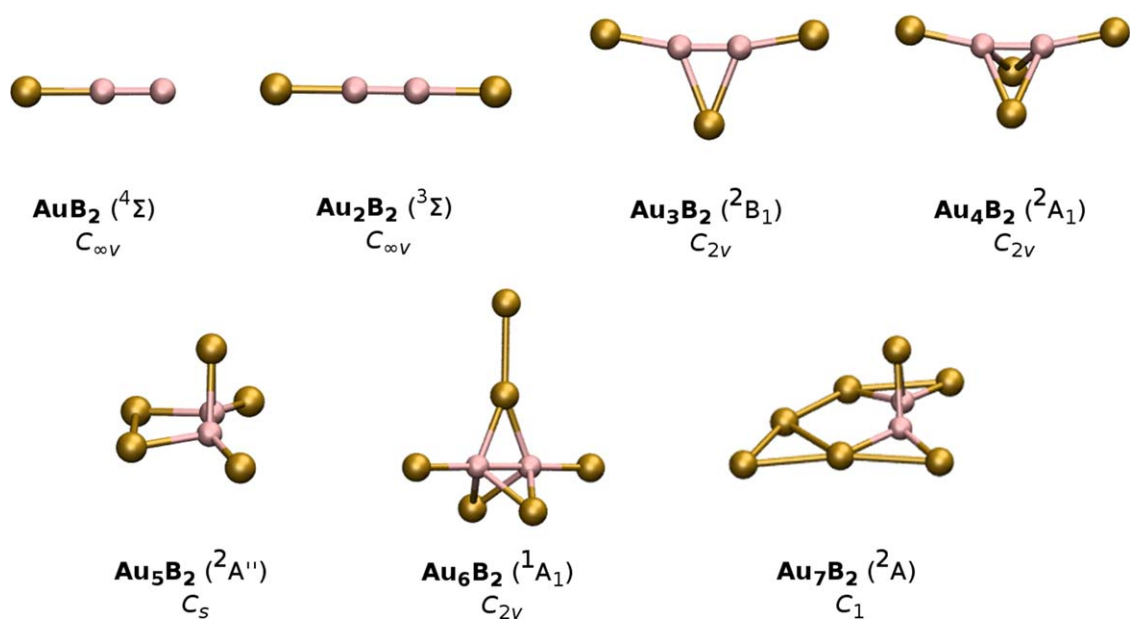

Figure 6. Global minimum structures of the Au_mB_2 ($m = 1$–7) clusters. [Color figure can be viewed in the online issue, which is available at wileyonlinelibrary.com.]

Au has a negative charge (−0.25 |e|). In Au_2B or bigger clusters, one expects also a positive charge on the boron atom. However, Figure 1-SI shows that this is not the case. In all the title clusters, boron has a negative charge (between −0.08 and −1.61 |e|), while the gold atoms bonded to boron are positively charged (0.04–0.45 |e|). The gold atoms out of the first coordination sphere have a negligible negative charge, except in Au_6B_2 (q(Au) = −0.21 |e|). The natural population analysis (NPA) charges documents the ionic bonding character of the gold–boron clusters, which has a strong repercussion in their reactivity (*vide infra*).

The case of AuB is intriguing. The Au—B bond length is 1.924 Å. This value is shorter than the average Au—B bond distance (2.039 Å). Li and Li suggested the presence of a triple

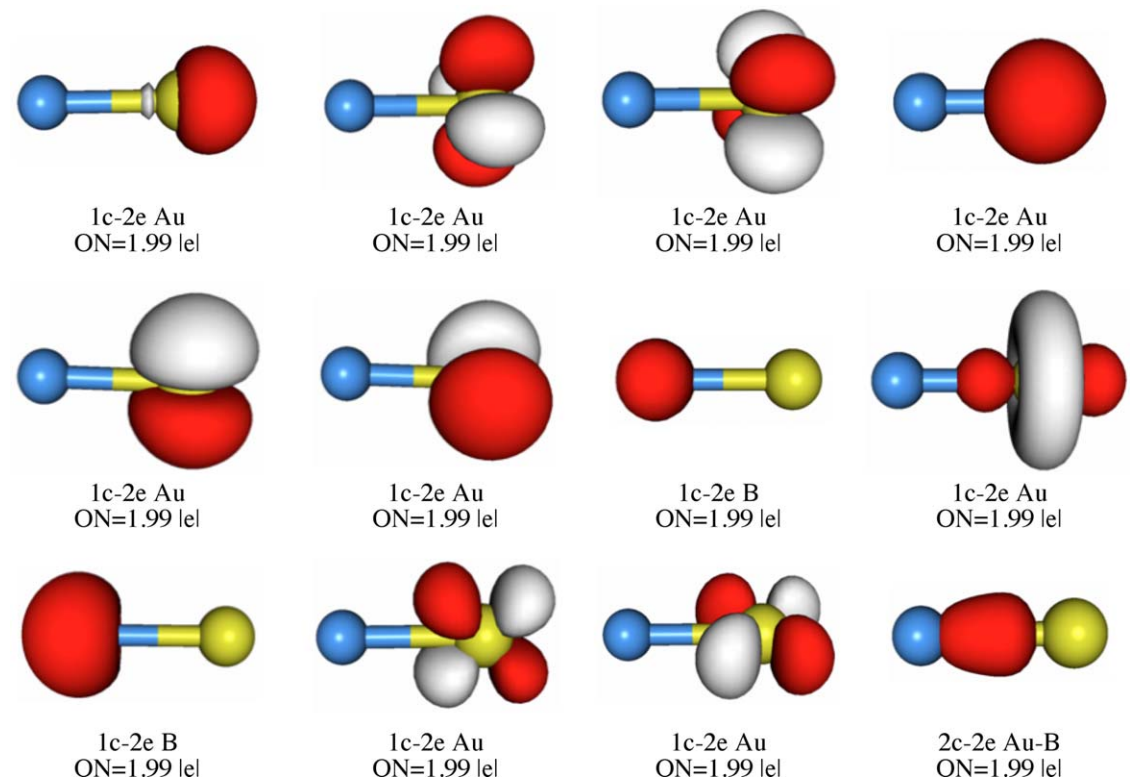

Figure 7. Bonds and lone pairs recovered by the AdNDP analysis for AuB. ON is the occupation number. [Color figure can be viewed in the online issue, which is available at wileyonlinelibrary.com.]

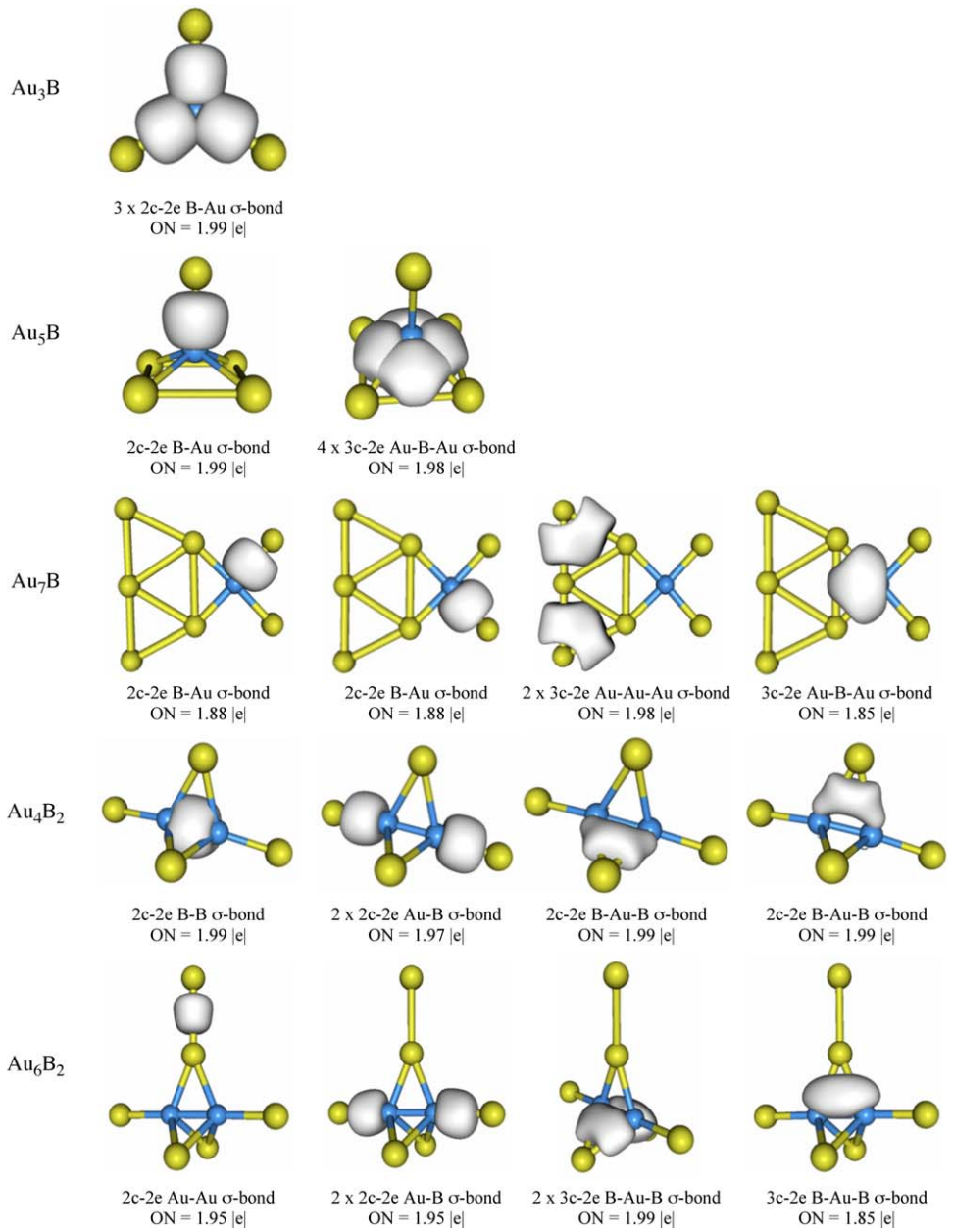

Figure 8. Bonds recovered by the AdNDP analysis for Au_3B, Au_5B, Au_7B, Au_4B_2, and Au_6B_2. ON is the occupation number. [Color figure can be viewed in the online issue, which is available at wileyonlinelibrary.com.]

bond, exclusively based on the distance.[17] However, the Wiberg bond index (WBI)[21] is only 1.30, indicating the presence of a single (perhaps a double) bond. To give an answer to this puzzle, a series of AdNDP computations were done. In the case of AuB, we consider not only the valence electrons in the analysis, the five electrons of boron, and the last 16 electrons of gold are also included in the computations (Fig. 7). Only one 2c-2e σ-bonding is found with an ON of 1.99 |e|. The other two valence electrons of boron are located as a lone pair. The electrostatic potential of AuB shows a negative region around the boron atom, supporting also the presence of a lone pair. These evidences support the existence of a short B—Au σ-bond in AuB.

For the rest of the Au—B clusters, Au—B WBIs show the Au—B bond order ranges from 0.37 for Au_6B_2 to 1.30 for AuB (see Supporting Information Figure 5-SI), indicating a significant Au—B bonding interactions. The total WBI of the boron atoms goes from 1.44 for AuB_2 to 4.05 for Au_5B, which implies the octet rule is not violated despite the hypercoordination in Au_nB ($n = 5$–8) and Au_6B_2. Note that the total WBI of gold atoms does not exceed the value of 2.

Unfortunately, the AdNDP analysis is available only for closed-shell systems. Nevertheless, Figure 8 summarizes the AdNDP results for Au_3B, Au_5B, Au_7B, Au_4B_2, and Au_6B_2. The bonding pattern in Au_3B, revealed by the AdNDP analysis, shows the presence of three 2c-2e Au—B σ-bonds, similar to that in borane.[22] In

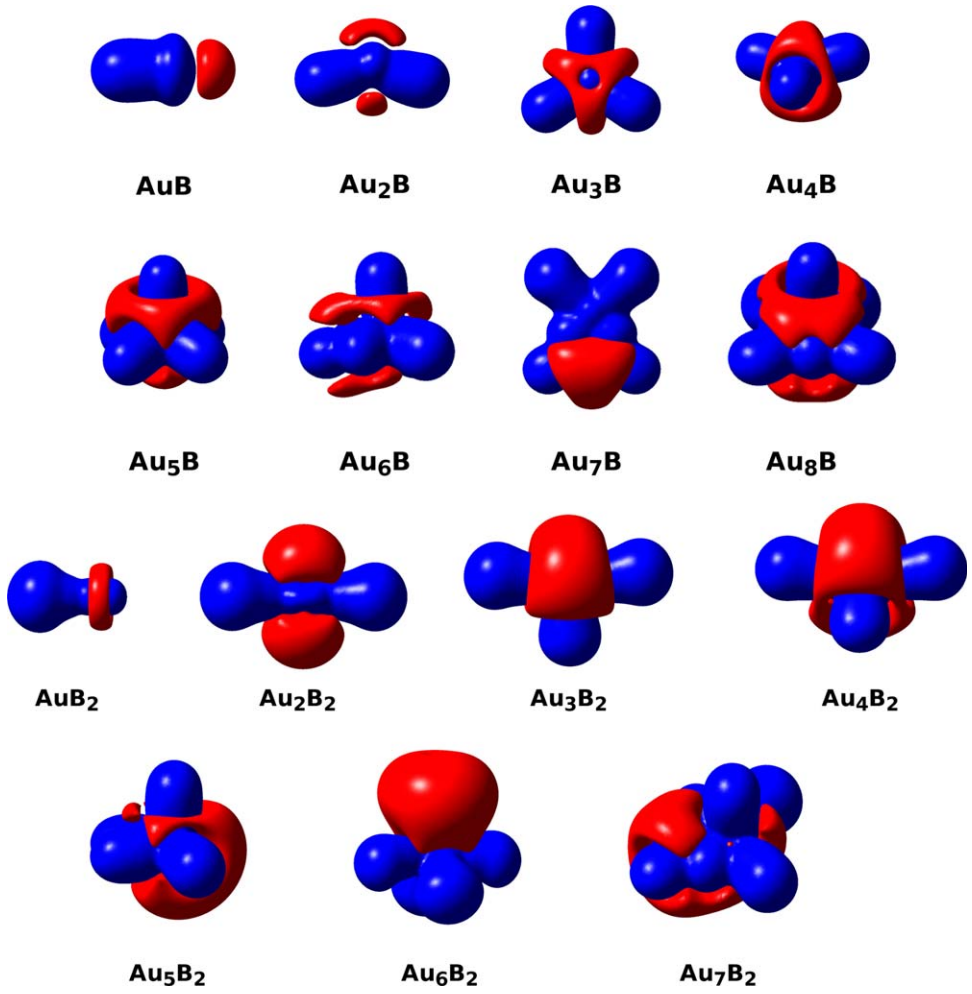

Figure 9. Electrostatic Potential Isosurfaces (|MEP| = 0.02 au) for the global minimum structures of Au_nB ($n = 1, 8$) and Au_mB_2 ($m = 1, 7$) clusters. [Color figure can be viewed in the online issue, which is available at wileyonlinelibrary.com.]

AuB_5, there is a 2c-2e Au—B σ-bond and four 3c-2e Au—B—Au σ-bonds, explaining why the apical Au—B bond length (2.005 Å) is shorter than the axial ones (2.111 Å). Despite boron atom is pentacoordinate, given the boron preference to form multicenter bonds, it does violate the octet rule, and thus, it should be classified as a hypercoordinate atom. Au_7B possesses a planar tetracoordinate boron atom, where boron is bounded to the peripheral atoms via two 2c-2e Au—B σ-bonds and one 3c-2e Au—B—Au σ-bond. Evidently, the former Au—B distance (2.020 Å) is shorter than the multicenter contact (2.086 Å). The gold fragment in Au_7B is stabilized by two 3c-2e σ-bond.

In Au_4B_2, the B—B bond is a single bond. While the Au—B bonds located parallel to the boron dimer are also 2c-2e σ-bonds, the bridged gold atoms are linked to the boron fragment via two 3c-2e B—Au—B σ-bonds. The bonding situation in Au_6B_2 is slightly different to Au_4B_2, because part of the electron density involved into the B—B bond is donated to form a 3c-2e B—Au—B interaction, clarifying why the B—B distance in Au_6B_2 (1.698 Å) is considerably longer than that computed in Au_4B_2 (1.586 Å). Finally, Au_4B_2 is the only one with a single Au—Au bond (2.551 Å).

Reactivity

The electrostatic potential has been used extensively as a local index of chemical reactivity. Location of positive and negative regions of this function has been used to identify the sites of nucleophilic and electrophilic attack, respectively.[23] It is particularly effective in relation to noncovalent interactions and early stages of chemical processes that involve bond formation and/or charge transfer. The substitution of one gold atom by boron modifies drastically the structure and reactivity. The electrostatic potential isosurfaces show that negative regions are accumulated around the boron fragments (see Fig. 9). This is more evident in the Au_mB_2 clusters. So, in the case of a CO oxidation, one can anticipate that carbon will interact with the boron fragment and oxygen with the gold skeleton.

Summary and Outlook

Our computations indicate that the global minimum of Au_nB ($n = 1$–8) and Au_mB_2 ($m = 1$–7) clusters do not have the same geometry as pure gold clusters. The substitution of one gold atom by boron modifies drastically the structure and reactivity.

Nevertheless, there are well-defined growth patterns. It is quite interesting that some structures have planar hypercoordinate boron atoms. The bond of these mixed clusters is explained via the presence of multicenter bonds. The electrostatic potential isosurfaces show that negative regions are accumulated around the boron fragments. So, in the case of a CO oxidation, one can anticipate that carbon will interact with the boron fragment and oxygen with the gold skeleton. These results are important for future applications and to improve the understanding of the extraordinary catalytic properties of gold nanostructures.

Acknowledgments

The CGSTIC (Xiuhcóatl) at Cinvestav and KanBalam at UNAM are gratefully acknowledged for generous allocation of computational resources. PRMA thanks DGAPA-UNAM for a postdoctoral fellowship.

Keywords: gold clusters · boron clusters · chemical bond · potential energy surfaces

How to cite this article: R. Grande-Aztatzi, P. R. Martínez-Alanis, J. L. Cabellos, E. Osorio, A. Martínez, G. Merino, *J. Comput. Chem.* **2014**, *35*, 2288–2296. DOI: 10.1002/jcc.23748

Additional Supporting Information may be found in the online version of this article.

[1] (a) W. A. Deheer, *Rev. Mod. Phys.* **1993**, *65*, 611; (b) P. Mulvaney, *Langmuir* **1996**, *12*, 788; (c) M. Haruta, *Catal. Today* **1997**, *36*, 153; (d) M. Valden, X. Lai, D. W. Goodman, *Science* **1998**, *281*, 1647; (e) S. Link, M. A. El-Sayed, *J. Phys. Chem. B* **1999**, *103*, 8410; (f) K. L. Kelly, E. Coronado, L. L. Zhao, G. C. Schatz, *J. Phys. Chem. B* **2003**, *107*, 668; (g) M. C. Daniel, D. Astruc, *Chem. Rev.* **2004**, *104*, 293; (h) G. Schmid, *Chem. Rev.* **1992**, *92*, 1709; (i) G. C. Bond, D. T. Thompson, *Catal. Rev. Sci. Eng.* **1999**, *41*, 319; (j) A. C. Templeton, M. P. Wuelfing, R. W. Murray, *Acc. Chem. Res.* **2000**, *33*, 27; (k) N. R. Jana, L. Gearheart, C. J. Murphy, *J. Phys. Chem. B* **2001**, *105*, 4065; (l) B. Nikoobakht, M. A. El-Sayed, *Chem. Mater.* **2003**, *15*, 1957; (m) C. J. Murphy, T. K. San, A. M. Gole, C. J. Orendorff, J. X. Gao, L. Gou, S. E. Hunyadi, T. Li, *J. Phys. Chem. B* **2005**, *109*, 13857; (n) B. D. Chithrani, A. A. Ghazani, W. C. W. Chan, *Nano Lett.* **2006**, *6*, 662; (o) Y. Y. Yu, S. S. Chang, C. L. Lee, C. R. C. Wang, *J. Phys. Chem. B* **1997**, *101*, 6661; (p) A. Sanchez, S. Abbet, U. Heiz, W. D. Schneider, H. Hakkinen, R. N. Barnett, U. Landman, *J. Phys. Chem. A* **1999**, *103*, 9573; (q) P. K. Jain, K. S. Lee, I. H. El-Sayed, M. A. El-Sayed, *J. Phys. Chem. B* **2006**, *110*, 7238.

[2] (a) S. Eustis, M. A. El-Sayed, *Chem. Soc. Rev.* **2006**, *35*, 209; (b) E. Roduner, *Chem. Soc. Rev.* **2006**, *35*, 583.

[3] (a) N. Lopez, T. V. W. Janssens, B. S. Clausen, Y. Xu, M. Mavrikakis, T. Bligaard, J. K. Norskov, *J. Catal.* **2004**, *223*, 232; (b) B. Yoon, H. Hakkinen, U. Landman, A. S. Worz, J. M. Antonietti, S. Abbet, K. Judai, U. Heiz, *Science* **2005**, *307*, 403; (c) A. A. Herzing, C. J. Kiely, A. F. Carley, P. Landon, G. J. Hutchings, *Science* **2008**, *321*, 1331; (d) Y. Gao, N. Shao, Y. Pei, Z. Chen, X. C. Zeng, *ACS Nano* **2011**, *5*, 7818; (e) L. D. Socaciu, J. Hagen, T. M. Bernhardt, L. Woste, U. Heiz, H. Hakkinen, U. Landman, *J. Am. Chem. Soc.* **2003**, *125*, 10437; (f) I. V. Yudanov, R. Sahnoun, K. M. Neyman, N. Rosch, J. Hoffmann, S. Schauermann, V. Johanek, H. Unterhalt, G. Rupprechter, J. Libuda, H. J. Freund, *J. Phys. Chem. B* **2003**, *107*, 255; (g) I. N. Remediakis, N. Lopez, J. K. Norskov, *Appl. Catal. A* **2005**, *291*, 13.

[4] P. Schwerdtfeger, *Angew. Chem. Int. Ed. Engl.* **2003**, *42*, 1892.

[5] (a) J. L. Wang, G. H. Wang, J. J. Zhao, *Phys. Rev. B* **2002**, *66*, 035418; (b) H. Hakkinen, B. Yoon, U. Landman, X. Li, H. J. Zhai, L. S. Wang, *J. Phys. Chem. A* **2003**, *107*, 6168; (c) J. Zhao, J. L. Yang, J. G. Hou, *Phys. Rev. B* **2003**, *67*, 085404; (d) L. Xiao, B. Tollberg, X. K. Hu, L. C. Wang, *J. Chem. Phys.* **2006**, *124*, 114309; (e) X.-B. Li, H.-Y. Wang, X.-D. Yang, Z.-H. Zhu, Y.-J. Tang, *J. Chem. Phys.* **2007**, *126*, 084505; (f) E. Apra, R. Ferrando, A. Fortunelli, *Phys. Rev. B* **2006**, *73*, 205414; (g) E. M. Fernandez, J. M. Soler, L. C. Balbas, *Phys. Rev. B* **2006**, *73*, 235433; (h) L. Ferrighi, B. Hammer, G. K. H. Madsen, *J. Am. Chem. Soc.* **2009**, *131*, 10605; (i) A. Pinto, A. R. Pennisi, G. Faraci, G. Dagostino, S. Mobilio, F. Boscherini, *Phys. Rev. B* **1995**, *51*, 5315; (j) I. L. Garzon, M. R. Beltran, G. Gonzalez, I. Gutierrez-Gonzalez, K. Michaelian, J. A. Reyes-Nava, J. I. Rodriguez-Hernandez, *Eur. Phys. J. D* **2003**, *24*, 105; (k) X. Li, B. Kiran, L. S. Wang, *J. Phys. Chem. A* **2005**, *109*, 4366; (l) Y. K. Han, *J. Chem. Phys.* **2006**, *124*, 024316; (m) B. Assadollahzadeh, P. Schwerdtfeger, *J. Chem. Phys.* **2009**, *131*, 064306; (n) L. M. Molina, J. A. Alonso, *J. Phys. Chem. C* **2007**, *111*, 6668; (o) A. Deka, R. C. Deka, *J. Mol. Struct. Theochem* **2008**, *870*, 83; (p) D. Y. Zubarev, A. I. Boldyrev, *J. Phys. Chem. A* **2009**, *113*, 866.

[6] A. Martinez, *J. Phys. Chem. C* **2010**, *114*, 21240.

[7] A. P. Sergeeva, A. I. Boldyrev, *J. Cluster Sci.* **2011**, *22*, 321.

[8] D. A. Goetz, R. Schaefer, P. Schwerdtfeger, *J. Comput. Chem.* **2013**, *34*, 1975.

[9] (a) C.-J. Wang, X.-Y. Kuang, H.-Q. Wang, H.-F. Li, J.-B. Gu, J. Liu, *Comput. Theor. Chem.* **2012**, *1002*, 31; (b) W. Bouwen, F. Vanhoutte, F. Despa, S. Bouckaert, S. Neukermans, L. T. Kuhn, H. Weidele, P. Lievens, R. E. Silverans, *Chem. Phys. Lett.* **1999**, *314*, 227; (c) M. Heinebrodt, N. Malinowski, F. Tast, W. Branz, I. M. L. Billas, T. P. Martin, *J. Chem. Phys.* **1999**, *110*, 9915; (d) C. Majumder, A. K. Kandalam, P. Jena, *Phys. Rev. B* **2006**, *74*; (e) D. Bhattacharjee, B. K. Mishra, A. K. Chakrabartty, R. C. Deka, *Comput. Theor. Chem.* **2014**, *1034*, 61; (f) Y. Romero, P. R. Martinez-Alanis, J. Rafael Leon-Carmona, A. Martinez, *Comput. Theor. Chem.* **2013**, *1021*, 35.

[10] D. Y. Zubarev, A. I. Boldyrev, *Phys. Chem. Chem. Phys.* **2008**, *10*, 5207.

[11] A. E. Reed, R. B. Weinstock, F. Weinhold, *J. Chem. Phys.* **1985**, *83*, 735.

[12] J. Cabellos, F. Ortiz–Chi, A. Ramírez, G. Merino, Bilatu 1.0, Cinvestav, Mérida, 2013.

[13] M. Matsumoto, T. Nishimura, *ACM T Model Comput. S* **1998**, *8*, 3.

[14] (a) C. Adamo, V. Barone, *J. Chem. Phys.* **1999**, *110*, 6158; (b) P. J. Hay, W. R. Wadt, *J. Chem. Phys.* **1985**, *82*, 299.

[15] F. Weigend, R. Ahlrichs, *Phys. Chem. Chem. Phys.* **2005**, *7*, 3297.

[16] M. J. Frisch, G. W. Trucks, H. B. Schlegel, G. E. Scuseria, M. A. Robb, J. R. Cheeseman, G. Scalmani, V. Barone, B. Mennucci, G. A. Petersson, H. Nakatsuji, M. Caricato, X. Li, H. P. Hratchian, A. F. Izmaylov, J. Bloino, G. Zheng, J. L. Sonnenberg, M. Hada, M. Ehara, K. Toyota, R. Fukuda, J. Hasegawa, M. Ishida, T. Nakajima, Y. Honda, O. Kitao, H. Nakai, T. Vreven, J. A. Montgomery, J. E. Peralta, F. Ogliaro, M. Bearpark, J. J. Heyd, E. Brothers, K. N. Kudin, V. N. Staroverov, R. Kobayashi, J. Normand, K. Raghavachari, A. Rendell, J. C. Burant, S. S. Iyengar, J. Tomasi, M. Cossi, N. Rega, J. M. Millam, M. Klene, J. E. Knox, J. B. Cross, V. Bakken, C. Adamo, J. Jaramillo, R. Gomperts, R. E. Stratmann, O. Yazyev, A. J. Austin, R. Cammi, C. Pomelli, J. W. Ochterski, R. L. Martin, K. Morokuma, V. G. Zakrzewski, G. A. Voth, P. Salvador, J. J. Dannenberg, S. Dapprich, A. D. Daniels, Farkas, J. B. Foresman, J. V. Ortiz, J. Cioslowski, D. J. Fox, Gaussian 09, Revision C.01; Gaussian: Wallingford, CT, **2009**.

[17] D.-Z. Li, S.-D. Li, *Int. J. Quantum Chem.* **2011**, *111*, 4418.

[18] A. C. Castro, E. Osorio, J. Luis Cabellos, E. Cerpa, E. Matito, M. Sola, M. Swart, G. Merino, *Chem. Eur. J.* **2014**, *20*, 4583.

[19] W.-Z. Yao, D.-Z. Li, S.-D. Li, *J. Comput. Chem.* **2011**, *32*, 218.

[20] P. Schwerdtfeger, *Chem. Phys. Lett.* **1991**, *183*, 457.

[21] K. B. Wiberg, *Tetrahedron* **1968**, *24*, 1083.

[22] H. J. Zhai, L. S. Wang, D. Y. Zubarev, A. I. Boldyrev, *J. Phys. Chem. A* **2006**, *110*, 1689.

[23] J. S. Murray, P. Politzer, *WIREs Comput. Mol. Sci.* **2011**, *1*, 153.

Received: 25 August 2014
Revised: 9 September 2014
Accepted: 11 September 2014
Published online on 3 October 2014